Calcitriol in Hedgehog signaling regulation

A functional and putative physiological role of calcitriol in Patched1/Smoothened interaction

### Benedikt Linder<sup>1</sup>, Susanne Weber<sup>2</sup>, Kai Dittmann<sup>3</sup>, Jerzy Adamski<sup>2</sup>, Heidi Hahn<sup>1</sup>, and Anja Uhmann<sup>1</sup>

<sup>1</sup>From the Institute of Human Genetics, Tumor Genetics Group, University Medical Center Goettingen, Germany
<sup>2</sup> From the Department Genome Analysis Centre, Institute for Experimental Genetics, Helmholtz Zentrum
Muenchen, National Research Center for Environment and Health, Neuherberg, Germany
<sup>3</sup> From the Institute of Cellular and Molecular Immunology, University Medical Center Goettingen, Germany

\*Running title: Calcitriol in Hedgehog signaling regulation

To whom correspondence should be addressed: Anja Uhmann, Institute of Human Genetics, University Medical Center Goettingen, Heinrich-Dueker-Weg 12, 37073 Goettingen, Germany; Phone: +49 551 3914100; Fax: +49 551 3966580; email: <a href="mailto:auhmann@gwdg.de">auhmann@gwdg.de</a>

**Key words:** Hedgehog/Patched1 signaling; calcitriol; 1α,25(OH)<sub>2</sub>D<sub>3</sub>; itraconazole; Smoothened

**Background:** Smoothened activity is mediated by a still undiscovered small molecule.

**Results:** Patched1 is required for calcitriol release and calcitriol inhibits Smoothened independently of the cysteine-rich-domain and seven-transmembrane-domain. **Conclusions:** Calcitriol exhibits excellent characteristics of a signal transduction molecule in Patched1/Smoothened interaction.

**Significance:** Understanding how Smoothened activity is regulated for new therapeutic options to fight Hedgehog-associated cancers.

### **ABSTRACT**

The Patched1 (Ptch)-mediated inhibition Smoothened (Smo) is still an open question. However, a direct Ptch/Smo interaction has been excluded, Smo modulators were identified, but the endogenous signal transmitting molecule remains undiscovered. Here, we demonstrate that calcitriol, the hormonally active form of vitamin D<sub>3</sub>, is an excellent candidate for transmission of Ptch/Smo interaction. Our study reveals that Ptch expression is sufficient to release calcitriol from the cell and that calcitriol inhibits Smo action and ciliary translocation by acting on a site distinct from the 7transmembrane-domain or the cysteine-rich-domain. Moreover calcitriol strongly synergizes itraconazole (ITZ) in Smo inhibition which not results from elevated calcitriol bio-availability due to ITZmediated 24-hydroxylase inhibition but rather from a direct interaction of the compounds at the level of Smo. Together, we suggest that calcitriol represents a possible endogenous transmitter of Ptch/Smo interaction. Moreover calcitriol or calcitriol derivatives combined with ITZ might be a treatment option of Hedgehogassociated cancers.

The Hedgehog (Hh) signaling pathway plays an essential role in cell differentiation, organ patterning, cell proliferation, stem cell maintenance and regenerative responses after injury (1-3). Aberrant Hh signaling during embryogenesis leads to birth defects whereas overactive Hh signaling in somatic cells of adults results in cancer formation (1). Thus, the exact knowledge about the regulation of the pathway's activity is highly important for a better understanding of Hh-associated tumorigenesis and the development of new anti-cancer therapies.

Most commonly affected in Hh-associated cancer formation is the interaction between the Hh receptor Patched1 (Ptch) and Smoothened (Smo) (4). In the absence of Hh proteins Ptch inhibits Smo due to an, so far, unknown catalytic mechanism (5-7). The binding of Hh to Ptch terminates the inhibition of Smo followed by the translocation of Smo into the primary cilium and by the activation of the Hh signaling cascade, which is characterized by transcription of Gli target genes (e.g., *Gli1*) (1,4).

Ptch consists of 12 hydrophobic transmembrane domains, the intracellular C- and N-terminal regions and two extracellular loops that mediate the binding of the Hh ligand (8,9). Five of the transmembrane domains form a domain resembling a sterol-sensing-domain (SSD) (10,11), a motif found in proteins which are involved in intracellular sterol-level sensing (12). The SSD is essential for the function of Ptch (13). According to the oligomeric structures of SSD-transporters Ptch proteins form stable trimers (14). Thus, it is tempting to speculate that Ptch is a multisubunit transporter whose activity indirectly regulates the function of Smo e.g., by pumping small sterol-like molecules Experiments from our and other laboratories foster this hypothesis since medium conditioned from wildtype (wt) *Ptch* cells but not from *Ptch*-mutant (*Ptch*<sup>-/-</sup>) cells has Smo-inhibitory properties. This suggests that *Ptch*<sup>-/-</sup> cells are either defective in the release (16,17) and/or in the synthesis of Smo-inhibitory molecules.

Ptch's signaling partner Smo consists of a 7transmembrane-domain (7TM), an intracellular Cterminal tail and an extracellular N-terminal region containing a cysteine-rich-domain (CRD) (18,19). The 7TM harbors a binding site for Smo inhibitors (e.g., cyclopamine (CP) (20), vismodegib (21)) and activators (Smoothened agonist; SAG (22,23)). Whereas no endogenous molecule has been identified that regulates Smo activity upon binding to the 7TM, endogenous derivatives of cholesterol (oxysterols) (15,24,25)such as 20(S)-hydroxycholesterol (20(S)OHC) can bind and activate Smo via its CRD (18,19).

Recently we described that the oxysterol calcitriol, a twice hydroxylated vitamin D<sub>3</sub> derivative, efficiently inhibits Hh signaling of *Ptch*-associated tumors and Hhstimulated wt *Ptch* and *Ptch*<sup>-/-</sup> cells (17,26). Moreover, we demonstrated that calcitriol inhibits Hh signaling downstream of Ptch but upstream of Gli supposedly at the level of Smo. Thus, calcitriol does not inhibit Hh signaling in *Smo*<sup>-/-</sup> cells, but efficiently inhibits Hh signaling after transfection with a SMO expression plasmid. Beyond that calcitriol inhibits Shh-induced Hh signaling activity in Vitamin D receptor (*Vdr*) knock out cells resembling a Vdr-independent mechanism of calcitriol-mediated Hh signaling inhibition (17).

Due to the facts that a) Ptch shows similarities to sterol transporters (10,11), b) *Ptch*-/cells are unable to secrete Hh-inhibitory factors (16,17), c) Smo activity is controllable by oxysterols (15,24,25) and d) the natural occurring oxysterol calcitriol efficiently inhibits Hh signaling (17,26) it is tempting to speculate that calcitriol might be an endogenous mediator of Ptch/Smo interaction and Smo inhibition.

In this study we analyzed the molecular mechanisms of the calcitriol-mediated inhibition of Hh signaling. Mass spectroscopic assays and media transfer experiments demonstrate that Ptch is dispensable for the synthesis of calcitriol from its precursor vitamin D<sub>3</sub>. However, it is essential for calcitriol release into the extracellular space. In addition, functional competition assays, fluorescence-based replacement studies and analysis of the activity of several Smo variants show that calcitriol does neither bind to Smo's 7TM nor to its CRD but efficiently inhibits the translocation of Smo into the primary cilia in *Ptch*<sup>-/-</sup> and SAG-treated 3T3/NIH cells. Beyond that the antitumoral effects of

calcitriol are strongly enhanced by itraconazole (ITZ) which was not induced by an ITZ-mediated elevated bio-availability of calcitriol but by a synergism of both compounds in Hh signaling inhibition.

Taken together, our results strengthened our hypothesis that calcitriol is a physiological regulator of Hh signaling activity. Moreover, this study opens new perspectives for combined calcitriol/ITZ-based therapies against Hh-associated cancers.

#### EXPERIMENTAL PROCEDURES

Compounds – Vitamin D<sub>3</sub> (Sigma-Aldrich, Germany), 25(OH)D<sub>3</sub> (25-hydroxy vitamin D<sub>3</sub>; Sigma-Aldrich), calcitriol (Sigma-Aldrich), CP (Toronto Research Chemicals Inc., Canada), BODIPY-labeled CP (BD-CP) (Toronto Research Chemicals) and 20(S)OHC (Tocris Bioscience, UK) were dissolved in ethanol (EtOH). ITZ (Sigma-Aldrich), SAG (Sigma-Aldrich) and vismodegib (GDC-0449) (Sellekchem, Texas, USA) were dissolved in DMSO. Tetracycline and sodium butyrate (Sigma-Aldrich) were dissolved in ddH<sub>2</sub>O and sterile filtrated. Final concentrations of all compounds are indicated in the respective experiments.

Cell lines – The fibroblast cell lines Smo<sup>-/-</sup>, Ptch<sup>-/-</sup> and the parental wt *Ptch* cells (see (17) for generation), the murine BCC cell line ASZ001 as well as the human keratinocyte cell line HaCaT are described in (17,27-29). NIH/3T3 cells were purchased from ATCC (CRL-1658). Shh light II cells represent NIH/3T3 cells stably transfected with a Gli-responsive firefly luciferase reporter and a constitutively expressed renilla luciferase (30). The tetracycline-inducible Smo-overexpressing cell line HEK293S was maintained as described in (24). Induction of ectopic Smo overexpression was performed according to (24) and was confirmed by western blot using anti-c-myc antibody (A-14, Santa Cruz). Shh-Nconditioned medium (Shh-N-CM) or respective control medium (CoM) were obtained from HEK293-Shh or HEK293 (ATCC; CRL-1537) cells, respectively, as described (22).

Plasmids – The plasmids pFR-Luc (Agilent Technologies, Santa Clara, CA, USA), pRL-CMV (Addgene; Cambridge, MA, USA), pGL-TK (Promega GmbH, Germany) and pEGFP-N1 (BD Bioscience, Germany) were purchased. The SMO and SMO-M2 expressing plasmids and the plasmids pCMV-BD-RXRα and pCMV-AD-VDR for the calcitriol-sensitive mammalian two hybrid (M2H) assay have been described previously (30-32).

For generation of wt Smo and  $Smo^{\Delta CRD}$  expression plasmids cherry-gene fused  $mSmo^{WI13Y}$  ( $mSmo^{WI13Y}$ -cherry) was amplified from the plasmid pHAGE

mSmo<sup>W113Y</sup>-cherry (19) by an overlap-extension PCR and subcloned into pMSCV (Takara Bio Europe/Clonetech, France). Afterwards the W113Y mutation was reversed to the wt Smo sequence using the QuikChange II XL-site-directed Mutagenesis-Kit (Agilent Technologies). To generate the Smo<sup>ACRD</sup> mutant plasmid the CRD sequence was deleted by an overlap-extension-PCR. Primer sequences are available upon request. The integrity of the subcloned and modified sequences was verified by Sanger sequencing.

Generation of Smo<sup>wt</sup> and Smo<sup>ΔCRD</sup> expressing cell lines – For generation of Smo<sup>wt</sup> or Smo<sup>ΔCRD</sup> expressing cells 50 % confluent Platinum E cells (kindly provided by M. Engelke, Institute of Cellular and Molecular Immunology, Goettingen, Germany) were transfected with 2.5 μg retroviral Smo<sup>wt</sup> and Smo<sup>ΔCRD</sup> expression plasmids in 400 μl culture medium of the target cell line and 5 μl Rotifect (Carl Roth GmbH + Co. KG, Germany). After 48 h the virus-containing supernatants were harvested, sterile-filtrated (0.45 μm pore size) and 2:1 diluted with culture medium of the target cell line. After the addition of 3 μg/ml polybrene (Sigma-Aldrich) this medium was applied to a 50 % confluent 5 cm dish of the target cell line. Next day the medium was changed and after additional 24 h 2 μg/ml puromycin was added to select for transduced cells.

Cell culture experiments – For gene expression analysis or Annexin V/propidium iodide assays (BD Biosciences, Germany) cells were seeded at densities of 40,000 or 240,000 cells/well in 24-well- or 6-well-plates, respectively. For 5-bromo-2'-deoxyuridine (BrdU) incorporation (Roche Diagnostics, Germany) or WST-1 (Roche life science, Germany) cells were seeded at densities of 8,000 or 7,000 cells/well in 96-well-plates, respectively. After 24 h, the cells were washed and incubated for additional 48 h with the respective growth medium supplemented with the compounds or solvent as indicated in the respective experiments. For ITZ treatment the culture medium was changed after 24 h to medium supplemented with 1.5% BSA (bovine serum albumin).

BrdU-pulse was conducted for the last 22 h of the incubation period. BrdU incorporation, WST-1 and Annexin V/propidium iodide assays were performed according to the manufacturer's instructions. BrdU incorporation and WST-1 assays were analyzed using a microplate reader (SynergyMX, BioTek Instruments, Inc.). Annexin V/propidium iodide assay was performed as described (33).

For gene expression analyses of NIH/3T3 150,000 cells were seeded per well of a 6-well-plate in DMEM containing 10% FCS and 1% PS. The following day the

treatment procedure was adopted from the protocol used for immunfluorescent-based detection of Smo accumulation in primary cilia (see below).

For analyzing ciliary localization of Smo NIH/3T3 or *Ptch*<sup>-/-</sup> cells were seeded in DMEM containing 10% FCS and 1% PS at a density of 250,000 cells per well of a 4 chamber CultureSlide (Falcon). After 7 h NIH/3T3 cells were starved for additional 24 h in DMEM containing 0.5% FCS and 1% PS followed by 16 h treatment in starvation medium containing the compounds or solvent as indicated in the respective experiments. *Ptch*<sup>-/-</sup> cells were treated 7 h after seeding without any additional starvation step for 16 h in starvation medium containing the compounds or solvent as indicated in the respective experiments.

For assaying the concentration-response curves (CRC) Shh light II cells were seeded in 96-wells plates at a density of 5,000 cells/well in growth medium. For the determination of CRC for one agonist and one antagonist of Hh signaling Shh light II cells were starved for 24 h in DMEM supplemented with 0.5% FCS and 1% PS one day after seeding. Treatments were conducted in DMEM containing 0.5% FCS. For the analysis of two Hh signaling inhibitors the cells were incubated in Shh-N-CM one day prior to the treatment. Treatments with the respective compounds or solvents were conducted in SHH-N-CM for 48 h. Afterwards dual-luciferase assays (Promega) were performed according to the manufacturer's instructions using a microplate reader (SynergyMX).

For transient transfection of *Smo*-- cells with *SMO* or *SMO-M2* expression plasmids 25,000 cells were seeded per well of a 24-well-plate. The next day the *Smo*-- cells were transfected with *SMO* or *SMO-M2* expression plasmids using a 3:1 ratio of Rotifect:DNA [μg] (Carl Roth) according to the manufacturer's instructions. After 24 h the transfected cells were treated with the compounds or solvent as indicated in the respective experiments.

Medium transfer experiments – For medium transfer experiments 2,000,000 wt Ptch or Ptch<sup>-/-</sup> cells were loaded with calcitriol by incubation in 10 ml prewarmed culture medium supplemented with 100 nM calcitriol or solvent for 1 h at 37°C in a 50 ml tube (Sarstedt AG & Co, Germany) rotating in a hybridization oven. After the loading procedure the cells were washed two times with 20 ml cold 1x PBS and seeded at a density of 200,000 cells/well in 6-well-plates in pre-warmed culture medium without calcitriol supplementation for 4, 6 or 8 h. Afterwards the conditioned medium was harvested and sterile filtrated. The same loading and conditioning procedure was

performed with supplemented medium without cells to control the adherence of calcitriol to the used plastic ware. Conditioned media from wt *Ptch* and *Ptch*<sup>-/-</sup> were stored at 4°C for up to one week (see Fig. 1b for procedure).

To analyze the calcitriol content of the conditioned media 200,000 NIH/3T3 cells/well were seeded in 6well-plates. The next day the cells were transfected with components of a mammalian two hybrid (M2H) system for assaying the heterodimerization of VDR and RXR\alpha (retinoic X receptor alpha) upon ligand binding (32). The firefly luciferase reporter vector (pFR-Luc), expression vectors encoding RXRα bait (pCMV-BD- $RXR\alpha$ ) and VDR prey (pCMV-AD-VDR) fusion constructs and pRL-TK were transfected in a ratio of 50:5:5:1 using a 3:1 ratio of Rotifect:DNA [µg] (Carl Roth). 6 h after transfection the cells were trypsinized and transferred to 96-well plates (70% confluency). The next day the transfected NIH/3T3 cells were incubated with 100 ul conditioned media from wt Ptch cells, Ptch<sup>-/-</sup> cells or no cell control for 16 h. Finally, dualluciferase assays (Promega) were performed according the manufacturer's instructions using a microplate reader (SynergyMX).

Flowcytometric-based replacement Flowcytometric-based replacement studies using BD-CP were performed in accordance with Chen et al.(20). In brief, ectopic Smo overexpression in HEK293S cells was induced by incubating cells grown to 70% confluency in DMEM/F12 (Life Technologies GmbH, Germany) supplemented with 10% FCS, 1% PS, 1 μg/ml tetracycline and 5 mM sodium butyrate for 48 h. Afterwards the cells were incubated for 4 h with the compounds as indicated in the respective experiments. Subsequently the cells were washed, trypsinized and centrifuged by 350x g for 8 min. The cells were washed again and resuspended in 350 to 500 µl phenol red-free DMEM (Life Technologies) supplemented with 0.5% FCS. Flowcytometric measurement was performed within 2 h on an LSR II flow cytometer (BD Bioscience). Per sample 50,000 cells were counted. Data acquisition and analysis was performed using the software BD FacsDiva (BD Biosciences Pharmingen) and FlowJo (Treestar Ashland). Experiments were performed in duplicates and repeated at least three times. The data were analyzed from the cumulative distribution function (CDF) which reflects the percentage fluorescenceintensity of cells. Each sample was normalized to BD-CP single-treated, tetracycline-induced cells (set to 100%). The respective bar graphs indicate the mean fluorescence intensity of each sample.

*Immunofluorescence staining* – Cells were fixed for 10 min with 2% paraformaldehyde at room temperature and for additional 5 min with methanol at -20°C. After permeabilization with 1x PBS containing 0.5% triton X-100 unspecific antigens were blocked with 4% BSA in 1x PBS containing 0.1% Tween-20 (PBST) for 1 h. Subsequently the cells were stained for 1 h with antiacetylated tubulin (Sigma-Aldrich, T6793, 1:500) and anti-Smo (Abcam, ab38686, 1:1000) antibodies. As secondary antibodies FITC-conjugated anti-mouse (Sigma-Aldrich, 1:200) and Cy3-labeled anti-rabbit antibodies (Jackson ImmunoResearch, 1:400) were used. Cells were mounted with ProLong Gold antifade reagent with DAPI (Life Technologies) and analyzed by fluorescence microscopy (Olympus BX60, equipped with U-RLF-T). Percentages of Smo positive cilia were calculated by counting all Smo positive and Smo negative primary cilia from at least six visual fields (600x magnification) of three independent experiments conducted in duplicates. Fluorescence images at 1000x magnification were acquiered by using a Color View camera (Soft Imaging System) and the software CellSens (Olympus Life Science, Germany). Images were processed with Adobe Photoshop CS5.

Reverse transcription and quantitative real time-PCR-analyses – Total RNA was extracted using TRIzol reagent (Life Technologies) according to the manufacturer's instructions. cDNA synthesis and primer combinations used for quantification of 18S rRNA, Gli1 and 25-hydroxy vitamin D<sub>3</sub>-24-hydroxylase (24-hydroxylase, Cyp24a1) transcripts by qRT-PCR were described previously (17,34,35). Gli1 and Cyp24a1 transcript levels were normalized to the transcript levels of 18S rRNA, after determining the respective amounts by the standard curve method. Each sample was measured in triplicates. Graphs represent the mean value of all measurements.

Mass spectroscopy of vitamin D<sub>3</sub> derivatives – For the detection of the vitamin D<sub>3</sub> metabolites vitamin D<sub>3</sub>, 24,25(OH)2D<sub>3</sub>, 25(OH)D<sub>3</sub> and calcitriol in cells, cell lysate extracts were analyzed via liquid chromatography coupled to tandem mass spectrometry (LC-MS/MS). Wt Ptch and Ptch<sup>-/-</sup> fibroblasts were seeded at a density of 200,000 cells/well in 6-well-plates. After starvation of the cells in FCS-free DMEM for 24 h the cells were treated with FCS-free DMEM supplemented with the respective compounds or solvents for the time points indicated in the respective experiments.

Afterwards, the medium was removed, cells were washed with 1x PBS and scraped using a 60% methanol/water (v/v) mixture supplemented with 40 ng/ml of internal standard 25-hydroxy vitamin  $D_2$ 

[25,26,27-<sup>13</sup>C<sub>3</sub>] (Cambridge Isotope Laboratories). Scraped cell/solvent suspensions were immediately transferred into a dry ice cooled reaction tube. The wells were rinsed again with 40% methanol/water (v/v). The cell lysates were stored at -80 °C until analysis.

Prior to LC-MS/MS analysis vitamin D<sub>3</sub> metabolites were extracted from the cell/solvent samples via offline solid phase extraction (SPE) using reversed phase based cartridges. LC-MS/MS analysis was performed by a 1260 HPLC system (Agilent Technologies) coupled to a QTrap5500 mass spectrometer (AB Sciex) which was controlled by Analyst 1.6 software (AB Sciex). The vitamin D<sub>3</sub> metabolites were baseline separated on a reversed phase column and detected by multiple reaction monitoring (MRM) after electrospray ionization (ESI).

In case of calcitriol, 24,25(OH)<sub>2</sub>D<sub>3</sub>, and 25(OH)D<sub>3</sub> three MRMs were monitored, whereas only one MRM was monitored for vitamin D<sub>3</sub>. The peaks of the respective vitamin D<sub>3</sub> metabolites (the sum of respective MRMs or the single MRM, respectively) were integrated by the Analyst 1.6 software and the areas were normalized by the peak area of the internal standard. The complete procedure will be published in detail elsewhere (manuscript in preparation).

Generation of concentration-response-curves (CRC) and Fa-CI-plots – CRC were calculated using GraphPad Prism 6 (GraphPad Software, La Jolla, CA, USA). For each individual sample the firefly-luciferase activity was normalized to the respective renilla luciferase value. Samples were normalized to solvent-treated controls which were set to 100%. Afterwards the values were logarithmized, the range of the data were normalized by setting the lowest and highest values to 0 and 100%, respectively, and the curves were fitted by non-linear regression using the log(inhibitor) vs. response – Variable slope (four parameters) or the respective log (agonist) function. Curve fitting was calculated using 1,000 iterations.

For generation of Fa-CI-plots the fractional inhibition (Fa) was calculated by normalizing to the data from 0 (lowest inhibition, i.e., solvent) to 1 (highest inhibition) and the combination index (CI) was calculated by the online software CompuSyn using the non-constant ratio setting (combosyn.com) (36). The data were plotted using GraphPad Prism 6.

Statistics – All statistical analyses were performed using GraphPad Prism 6. Statistical differences in ED<sub>50</sub> or Fa-CI-plots were calculated by the extra sum-of-squares F-test. No constrain or weighing was applied. Results from the M2H-assays, assays using Shh light II or Smo<sup>-/-</sup> cells and analyses of ciliary Smo accumulation were corrected for outliers using the ROUT-method

(Q=1%). After verification of Gaussian distribution by the D'Agostino & Pearson omnibus normality test one-way ANOVA using the Holm-Sidak's multiple comparison test or Dunnett's multiple comparisons test were conducted. The combination treatments of ASZ001 cells were tested using a non-parametric one-way ANOVA test (Kruskal-Wallis test). All other results were tested using a non-parametric Mann-Whitney test.

#### **RESULTS**

Ptch is required for the extracellular availability of calcitriol but dispensable for the synthesis from its precursors – We first investigated whether calcitriol is produced and released from Ptch-expressing cells. During calcitriol synthesis vitamin D<sub>3</sub> is mainly hydroxylated to 25(OH)D<sub>3</sub> by the vitamin D 25-This is followed hydroxylase (*Cyp27a1*). hydroxylation of  $25(OH)D_3$  to calcitriol by the  $1\alpha$ hydroxylase (Cyp27b1) (37). To examine if Ptch expression is required for the synthesis of calcitriol from its precursor vitamin D<sub>3</sub> we quantified the intracellular levels of vitamin D<sub>3</sub>, 25(OH)D<sub>3</sub> and calcitriol in wt Ptch and Ptch-'- fibroblasts after vitamin D<sub>3</sub> supplementation using mass spectrometric analyses (MS) experimental procedures). In both cell lines significantly elevated intracellular vitamin D<sub>3</sub> levels were already measured after 0.5 h (Fig. 1a). Intracellular vitamin D<sub>3</sub> levels peaked after 1 h, declined thereafter to a plateau and remained stable until 6 h after its supplementation (Fig. 1a). Intracellular 25(OH)D<sub>3</sub> was first detected after 1 h vitamin D<sub>3</sub> supplementation in wt Ptch cells and after 0.5 h in Ptch<sup>-/-</sup> cells (Fig. 1a). It significantly and continuously increased until the last time point at 6 h (Fig. 1a). Significant hydroxylation of 25(OH)D<sub>3</sub> to calcitriol was detected for the first time 4 h after vitamin D<sub>3</sub> treatment start in wt *Ptch* cells and after 2 h in *Ptch*<sup>-/-</sup> cells (Fig. 1a). Both cell lines showed a continuous increase of intracellular calcitriol levels that, compared with the 0.5 h value, reached significance after 6 h (Fig. 1a).

Since the experiments revealed that both wt Ptch and  $Ptch^{-/-}$  cells synthetize calcitriol from its precursor vitamin  $D_3$  and showed comparable vitamin  $D_3$  uptake and catalytic behavior we concluded that Ptch is dispensable for calcitriol synthesis.

We next analyzed if wt *Ptch* and *Ptch*-fibroblasts differ in their calcitriol releasing features by analyzing conditioned media from the respective cell lines. Without supplementation of calcitriol or its precursors endogenous calcitriol levels of *in vitro* cultured cells are very low and not detectable by non-derivatized MS (manuscript in preparation). Therefore, we first loaded

both cell lines with calcitriol. After thorough washing steps, the cells were cultured in calcitriol-free media. Thereupon the media were analyzed for its ability to promote recruitment of the VDR co-receptor, RXRα (retinoic acid receptor alpha), in a M2H reporter system (Fig. 1b; see experimental procedures) which is a very robust and highly sensitive read-out for calcitriol levels (Fig. 1c). Medium conditioned by calcitriolloaded wt *Ptch* cells highly induced the activation of VDR/RXRα heterodimerization whereas medium from calcitriol-loaded Ptch-/- cells was incapable to induce this to a comparable extend (Fig. 1d). Only a minimal activation of the M2H reporter assay by media from Ptch<sup>-/-</sup> fibroblasts was observed (Fig. 1d), which might rather reflect unspecific membrane shuttling of calcitriol then active transport through the cell membrane of Ptch-/- cells.

These data demonstrate that *Ptch*<sup>-/-</sup> cells, despite their ability to synthetize calcitriol from its precursor vitamin D<sub>3</sub>, lose their properties to release calcitriol to the extracellular space. Together with the fact that calcitriol efficiently inhibits Hh signaling at the level of Smo in a Vdr-independent manner (17) these data strengthened the hypothesis that calcitriol is a signal transducing molecule, which transfers Hh signaling inhibiting signals from Ptch to Smo.

Calcitriol efficiently inhibits the translocation of Smo into and facilitates the removal of Smo from the primary cilium — One of the earliest hallmarks of Hh signaling pathway activation (e.g. by Shh or SAG) is the accumulation of Smo in the primary cilium (38). Since our previous work has shown that calcitriol efficiently decreases Gli1 transcription as a marker of reduced Hh signaling activity (17) (see also Fig. 2a) we analyzed if calcitriol is also capable to prevent ciliary translocation of Smo upon Hh signaling activation.

Hence Smo localization in the primary cilia of solvent-, calcitriol-, SAG-, SAG/calcitriol-SAG/vismodegib-treated NIH/3T3 cells were visualized by double-immunofluorescence using anti-acetylated tubulin and anti-Smo antibodies. SAG treatment resulted in a strong ciliary localization of Smo, whereas calcitriol and vismodegib significantly reduced the SAG-induced recruitment of Smo into the cilia (Fig. 2b and c). Similar results were obtained after calcitriol treatment of Shhinduced NIH/3T3 cells (data not shown). Beyond that we also tested the effect of calcitriol on ciliary localization of Smo in Ptch-- cells which show a constitutive ciliary accumulation of Smo (Fig. 2d and e) and thus a constitutive pathway activation (17). Interestingly, 10 nM calcitriol were as potent as 1 µM

vismodegib in reducing the accumulation of Smo in the primary cilia (Fig. 2d and e).

These data show that calcitriol regulates ciliary translocation of Smo. Moreover, since calcitriol also promotes the removal of Smo from the cilia in *Ptch*-/cells these results confirmed our previously made observations that calcitriol acts at the level of Smo.

Calcitriol efficiently inhibits CRD-deleted Smo – The CRD of Smo has been described as an exclusive binding site for oxysterols that are discussed to be physiological regulators of Hh signaling activity (18,19). To analyze if calcitriol inhibits Hh signaling by binding to the CRD we generated Shh light II or  $Smo^{-/-}$  cell lines stably expressing wt Smo or a CRD-deleted variant  $(Smo^{\triangle CRD})$ .

In contrast to untransduced cells, wt Smo or Smo<sup>ΔCRD</sup>-expressing Shh light II cells showed a 5 to 10fold higher basal Hh reporter activity, which was barely increased by SAG or Shh treatment (Fig. 3a, b). Similar observations have been made by Myers et al. (39). Nevertheless the high Hh signaling activation of wt Smo or Smo<sup>ACRD</sup>-expressing cells enabled us to test the Hh signaling inhibiting properties of calcitriol without binding of activating molecules to Smo that may have preoccupied potential calcitriol binding sites. Both, calcitriol and CP treatment resulted in a significant inhibition of Hh signaling in SAG or Shh-treated untransduced Shh light II cells as well as in wt Smo and  $Smo^{\triangle CRD}$ -expressing Shh light II cells. However, compared to CP, the inhibitory effects of calcitriol were much more efficient in all settings (Fig. 3c, d). Similar results were obtained by Gli1 expression analyses of calcitriol or CP-treated wt Smo or Smo<sup>ΔCRD</sup>-expressing Smo<sup>-/-</sup> cells, which do not express endogenous Smo (Fig. 3e. f). Moreover, calcitriol was also capable to inhibit Hh signaling in Smo<sup>-/-</sup> cells expressing the constitutively active SMO-M2 variant (Fig. 3g) (31).

These data suggest that Hh signaling inhibition by calcitriol is not mediated by the binding to the oxysterol binding site of Smo (i.e. the CRD) or the SMO-M2 mutation site.

ITZ enhances the antitumoral potential of calcitriol – Calcitriol efficiently inhibits Hh signaling and proliferation and stimulates differentiation processes in *Ptch*-associated cancers in mice (17,26). Moreover, the inhibitory effect of calcitriol on Hh signaling is still detectable when Hh signaling is constitutively activated due to the expression of the oncogene SMO-M2 (Fig. 3g). These facts suggest that calcitriol might be an attractive candidate for the development of therapies against Hh-associated tumors. Thus we tested if the antitumoral effects of calcitriol could be enhanced by a

combination with the potent Smo-inhibitor ITZ (40) or with CP that binds Smo almost exclusively at the 7TM (18).

Single calcitriol, ITZ or CP treatments of the murine basal cell carcinoma cell line ASZ001 efficiently inhibited Hh signaling activity as revealed by reduced Gli1 mRNA expression (Fig. 4a, d, g). Although single calcitriol or ITZ treatments using BSA supplemented media did not significantly alter BrdU incorporation (Fig. 4c, i), the combined calcitriol/ITZ treatment significantly decreased both proliferation rate and Hh signaling activity (Fig. 4a, c). This was accompanied by a significant increase in the expression of the Vdrdowstream target Cvp24a1 indicating that ITZ enhances the Vdr-activating properties of calcitriol (Fig. 4b). In contrast, the combined treatments with calcitriol/CP (Fig. 4d-f) or CP/ITZ (Fig. 4g-i) did not lead to cooperative effects. Since effectiveness of ITZ-mediated Hh signaling inhibition is quenched by FCS (40) (own observations), ITZ treatment was conducted under serum starvation whereas calcitriol/CP-treated cells were cultured in media containing 2% FCS (please note the differences in calcitriol-mediated inhibition of proliferation under FCS-starved (Fig. 4c) and 2% FCS conditions (Fig. 4f)).

Changes in mitochondrial activity or apoptosis were not seen upon any of the treatments (data not shown).

Together these data suggest that the enhanced effects of the calcitriol/ITZ treatment on cellular proliferation and Hh signaling activity could be either based on a modification of the bio-availability of calcitriol, a direct interplay of the compounds in Hh signaling inhibition or a combination of both mechanisms.

ITZ does not influence calcitriol bio-availability -Azoles have been reported to inhibit the activity of cytochrome P450 enzymes, like the calcitriol-degrading 25-hydroxy D<sub>3</sub>-24-hydroxylase (24vitamin hydroxylase, Cyp24a1) (41,42). We therefore tested if ITZ might enhance the bio-availability of calcitriol by inhibition of Cyp24a1. If this would be the case, a calcitriol/ITZ treatment should result in increased intracellular calcitriol levels compared to single calcitriol treatment. Unfortunately, it was not possible to measure the calcitriol degradation product 1α,24,25(OH)<sub>3</sub>D<sub>3</sub> by non-derivatized MS-based assays in our hands. However, since Cyp24a1 also catalyzes the degradation of 25(OH)D<sub>3</sub> to 24,25-dihydroxy vitamin  $D_3$  (24,25(OH)<sub>2</sub> $D_3$ ) (37,43) we assumed that an ITZ-mediated inhibition of Cyp24a1 activity should also lead to a delayed 25(OH)D<sub>3</sub> degradation and to reduced 24,25(OH)<sub>2</sub>D<sub>3</sub> levels. To follow this line of investigation

we incubated ASZ001 cells with 25(OH)D<sub>3</sub> and ITZ and determined the intracellular 25(OH)D<sub>3</sub> 24,25(OH)<sub>2</sub>D<sub>3</sub> levels by LC/MS-MS analyses. This revealed the approach that combination 25(OH)D<sub>3</sub>/ITZ did neither result in significantly increased 25(OH)D<sub>3</sub> levels nor in reduced 24,25(OH)<sub>2</sub>D<sub>3</sub> levels when compared to 25(OH)D<sub>3</sub> treatment (Fig. 5a, b). In addition, ITZ did not influence the bio-availability of calcitriol in the cells, since the calcitriol levels were comparable after single calcitriol and the combined calcitriol/ITZ treatment (Fig. 5c). Similar results were obtained in HaCaT cells (data not shown) that have an intact vitamin D<sub>3</sub> metabolism (44).

Together, these data indicate that the combined effect of a calcitriol/ITZ treatment was not a result of delayed calcitriol degradation due to an ITZ-mediated Cyp24a1 inhibition.

Calcitriol and ITZ synergize in Smo-inhibition -Since calcitriol and ITZ are efficient inhibitors of the Hh signaling pathway at the level of Smo (17,40) we next tested if these compounds might inhibit Hh signaling synergistically. For this purpose we generated concentration-response curves (CRC) of calcitriol in the presence of ITZ or other known Smo modulating molecules using Shh light II cells. Neither increasing amounts of the Hh signaling activators SAG and 20(S)OHC or the inhibitors CP and vismodegib altered the IC<sub>50</sub> of calcitriol significantly (Fig. 6a-d; Table 1). Vice versa increasing amounts of calcitriol did not impact the half maximal effective dose (ED<sub>50</sub>) of CP, vismodegib, SAG or 20(S)OHC (Table 2, CRC not shown). In contrast, increasing amounts of ITZ shifted the half maximal inhibitory concentration (IC<sub>50</sub>) of calcitriol significantly from ~1.02 to ~0.13 nM (Fig. 6c; Table 1). Similar results were obtained for the IC<sub>50</sub> of ITZ in presence of increasing calcitriol concentrations (IC<sub>50</sub> shift of ITZ from  $\sim$ 0.81 to  $\sim$ 0. 59  $\mu$ M; Table 2). Analysis of the combination index (CI) (36) furthermore revealed that the combination of low calcitriol amounts (0.5 to 2.5 nM) with low, moderate and high ITZ concentrations resulted in a synergistic inhibition of Hh signaling in Shh light II cells (Fig. 6d).

Since none of the exclusive 7TM (vismodegib, SAG) or CRD (20(S)OHC) binders influenced calcitriol's IC<sub>50</sub> and thus did not compete with calcitriol for the binding of Smo at these sites, we assumed that calcitriol occupies an alternative Smo binding site. In addition, the synergistic inhibition of Hh signaling by calcitriol and ITZ indicated that calcitriol and ITZ bind to different Smo sites. To validate the hypothesis that calcitriol binds to Smo outside the 7TM or CRD, we tested if calcitriol or ITZ might compete for direct Smo

binding with BODIPY-labeled CP (BD-CP) in HEK293S cells (20,24), because the binding sites of CP have been already mapped to Smo's 7TM and to some extend to the CRD (18,20). Indeed, the known 7TM binders CP (Fig. 7a), SAG (data not shown) and vismodegib (data not shown) competed with BD-CP for Smo binding. The CRD binder 20(S)OHC also showed some competition with BD-CP, but to a lesser extent (Fig. 7d). This competition could be attributed to the weak binding capabilities of CP to the CRD (18). When ITZ was used, we found that it replaced significant amounts of Smo-bound BD-CP (Fig. 7b). This observation is different from that published by Kim et al. (40) and shows that ITZ binds to some extend either to the CRD or 7TM of Smo. In strong contrast, neither vitamin D<sub>3</sub>, 25(OH)D<sub>3</sub> (data not shown) nor high concentrations of calcitriol (20 nM =  $\sim 20x$  IC<sub>50</sub>) replaced BD-CP (Fig. 7c).

Taken together, these data demonstrate that calcitriol and ITZ synergize in Hh signaling inhibition, which might be due to the occupancy of different Smo binding sites by both drugs i.e., ITZ may occupy the 7TM or CRD of Smo whereas calcitriol or its precursors (vitamin  $D_3$  or  $25(OH)D_3$ ) may occupy Smo to a hitherto undefined binding site.

### **DISCUSSION**

Previous studies implicated the existence of small naturally-occurring oxysterols, whose availability is controlled by Ptch-mediated transport and that activate Smo by binding to the CRD (6,18,19,45,46). However, studies showing that Shh-induced activation of Hh signaling results in internalization of Shh-bound Ptch (14,47) questions this prediction, since loss of membrane associated Ptch should also result in loss of secretion of Smo-activating molecules. Therefore, it rather seems feasible that Ptch may secrete a negative regulator of Smo-activity. Indeed, vitamin D<sub>3</sub> or its derivatives may potentially fulfill the requirements for such a molecule (16,17,48,49). However, the direct proof and evidence for those assumptions are still missing (18,19,39).

In this study we provide evidence that calcitriol, a physiologically existing oxysterol, meets the characteristics of a Ptch/Smo signal transmitter molecule that is secreted by Ptch and negatively regulates Smo activity. First, we demonstrate that calcitriol is endogenously synthetized from its precursor vitamin  $D_3$  in adult fibroblasts. The synthesis does not require the presence of Ptch, because the increase of intracellular calcitriol after vitamin  $D_3$  supplementation was comparable in wt Ptch and  $Ptch^{-/-}$  fibroblasts. Since

several cell types have been reported to express Cyp27b1, which catalyzes the hydroxylation of 25(OH)D<sub>3</sub> to calcitriol (50), this finding was not surprising. Secondly, in line with previous findings that Ptch<sup>-/-</sup> cells are unable to secrete factors with Smoinhibitory properties (16,17), we found that media conditioned by wt Ptch cells significantly induced heterodimerization whereas VDR/RXRα conditioned by Ptch<sup>-/-</sup> cells did not. Since the M2H reporter assay is specifically activated in the presence of the VDR ligand calcitriol (see Fig. 1c) these results show that Ptch is required for calcitriol release from cells. Together we conclude that albeit Ptch-deficient cells are able to synthetize calcitriol from its precursor vitamin D<sub>3</sub> these cells are incapable to secrete it.

Several reports demonstrated the binding of Smoactivating oxysterols to Smo's CRD (18,19,39). This fascinating fact raises the question if this binding pocket might also be a target site for Smo-inhibiting molecules, like calcitriol (17,26). Nevertheless a study by Myers et al. suggested that neither the CRD nor the 7TM are the major sites of regulation by Ptch (39). Additionally the authors discussed that oxysterols like 20(S)OHC or 7ketocholesterol derivatives are unlikely to subserve the regulatory functions of Ptch (39). In accordance with this hypothesis our novel data provide evidence that neither the CRD nor the 7TM are required for calcitriol binding or calcitriol-mediated Smo inhibition. This conclusion is based on the finding that calcitriolmediated inhibition of Hh signaling can still be observed in cells expressing Smo<sup>ACRD</sup>. Moreover, we show that calcitriol does not compete with BD-CP, that is known to bind to the 7TM and to a lesser extend to the CRD (18). The assay furthermore revealed that the calcitriol precursors vitamin D<sub>3</sub> and 25(OH)D<sub>3</sub>, also did not compete with BD-CP for Smo binding. This is in contrast to Bijlsma et al. who showed the contrary (16). However, since all other compounds (i.e., SAG (22); vismodegib and 20(S)OHC (18); ITZ (40)) in our set up

showed the described competition with BD-CP we conclude that neither calcitriol nor its precursors bind to the CRD or the 7TM of Smo. Our data furthermore show that calcitriol acts as a non-competitive inhibitor for SAG and 20(S)OHC-induced Hh signaling activity since calcitriol reduced the maximal degree of Hh pathway activation of both compounds (Fig. 6e, f) without changing the respective ED<sub>50</sub> (Table 1, Table 2). This again fosters the assumption that calcitriol binds Smo at a site different from the CRD or 7TM (39,40). Finally, the observation that calcitriol is capable to inhibit the activity of mutant SMO-M2 which is mapped to the CP-binding pocket (30) strengthened the conclusion that calcitriol acts not at the 7TM.

We also discovered a synergistic inhibition of Hh signaling activity when combining calcitriol with the antifungal azole and Smo inhibitor ITZ (40). Azoles have been reported to inhibit the activity of cytochrome P450 enzymes (41,42). However, Kim et al. excluded an ITZ-mediated cytochrome P450 regulation, which is implicated in cholesterol biosynthesis (40). Similarly our data suggest that ITZ does not inhibit the calcitrioldegrading 24-hydroxylase. Indeed combined calcitriol/ITZ treatment led to a significantly higher Cyp24a1 expression compared to single calcitrioltreated cells (Fig. 4b). Contrary, our MS-based measurements demonstrated that calcitriol/ITZ treatment did not result in significant differences of calcitriol or 24,25(OH)<sub>2</sub>D<sub>3</sub> levels compared to single calcitriol-treated cells and that the level of intracellular 25(OH)D<sub>3</sub>, which likewise is degraded by the 24hydroxylase, was not influenced. However, due to the fact that enhanced Cyp24a1 expression levels rather reflects the general activation of Vdr signaling but does not measure the enzymatic activity of the 24hydroxylase these results suggested that ITZ might induce Vdr signaling via a separate mechanism but not due to interference of calcitriol catabolizing enzyme activity (e.g. 24-hydroxylase). Thus, we propose that the combined calcitriol/ITZ effects on Smo inhibition are not the result of an ITZ-mediated increase in calcitriol levels.

Besides, ITZ has been suggested to act and inhibit Smo at a site distinct from the CP binding pocket (40). This conclusion is based on the finding that ITZ competes barely with BD-CP for Smo binding (40). However, in our experiments BD-CP, which binds the 7TM as well as the CRD (18), was efficiently replaced by ITZ. Together with the fact that the IC<sub>50</sub> of ITZ is not affected by the CRD-binder 20(S)OHC (25) and ITZ act as a non-competitive inhibitor of Hh signaling activity induced by the CRD-binder SAG (40), we propose that ITZ rather binds to the 7TM than to the CRD. This assumption is furthermore strengthened by our findings that ITZ competes with BD-CP binding on Smo.

Calcitriol on the other hand does not compete with BD-CP for Smo binding and represents a non-competitive inhibitor of SAG and 20(S)OHC-induced Hh signaling activation. Furthermore it does not synergize with the 7TM binder CP or vismodegib in Smo inhibition. Thus, although we did not demonstrate direct binding of calcitriol to Smo we conclude that calcitriol binds to a Smo site distinct from the 7TM or CRD. This also could explain the synergistic effects with ITZ on Hh signaling inhibition. However, we have to admit that there is still the possibility that calcitriol inhibits Smo's action and ciliary accumulation by other indirect mechanisms.

Finally, our novel findings that ITZ as well as calcitriol synergistically inhibit Hh signaling may open new perspectives in the treatment of Hh-associated cancers, especially since both compounds are currently being tested in clinical trials for Hh-associated tumors (NCT02120677; NCT01358045). Indeed prospective experiments are needed to optimize the doses of both drugs and to elucidate the functional mechanisms of calcitriol/ITZ synergy in Hh signaling inhibition.

**Acknowledgement**: We thank J. Taipale (University of Helsinki, Finland) for providing of *Smo*<sup>-/-</sup> fibroblasts, E. Epstein (UCSF, USA) for the BCC cell line ASZ001, N. Sever (Stanford School of Medicine, USA) for HEK293S cells, M. Engelke (Institute of Cellular and Molecular Immunology, Goettingen, Germany) for help with and providing the cells and vector for retroviral transduction, D. Salic (Harvard Medical School, USA) for the *pHAGE mSmo* plasmids, P. Jurutka (School of Mathematical and Natural Sciences, Arizona State University, USA) for the *pCMV-BD-RXRα* and *pCMV-AD-VDR* (M2H) plasmids, and R. Toftgard (Karolinska Institute, Huddinge, Sweden) for the *SMO* and *SMO-M2* plasmids. This work was supported by grants of the Deutsche Forschungsgemeinschaft UH 228/2-1 and UH228/2-2 to AU.

Conflict of interests: The authors declare that they have no conflicts of interests with the contents of this article.

**Author contributions:** BL designed, performed and analyzed the experiments, wrote the paper and contributed to the preparation of the figures. AU conceived and coordinated the study, designed the experiments, analyzed data, wrote the paper and contributed to the preparation of the figures. SW established, performed and analyzed MS-based measurements of vitamin D<sub>3</sub> derivatives. KD designed and performed flowcytometric-based replacement studies. JA analyzed data, contributed vital reagents and analytical tools. HH contributed vital reagents and analytical tools and wrote the paper. All authors reviewed the results and approved the final version of the manuscript.

#### REFERENCES

- 1. Hooper, J. E., and Scott, M. P. (2005) Communicating with Hedgehogs. *Nature reviews. Molecular cell biology* **6**, 306-317
- 2. Machold, R., Hayashi, S., Rutlin, M., Muzumdar, M. D., Nery, S., Corbin, J. G., Gritli-Linde, A., Dellovade, T., Porter, J. A., Rubin, L. L., Dudek, H., McMahon, A. P., and Fishell, G. (2003) Sonic hedgehog is required for progenitor cell maintenance in telencephalic stem cell niches. *Neuron* 39, 937-950
- 3. Shin, K., Lee, J., Guo, N., Kim, J., Lim, A., Qu, L., Mysorekar, I. U., and Beachy, P. A. (2011) Hedgehog/Wnt feedback supports regenerative proliferation of epithelial stem cells in bladder. *Nature* **472**, 110-114
- 4. Briscoe, J., and Therond, P. P. (2013) The mechanisms of Hedgehog signalling and its roles in development and disease. *Nature reviews. Molecular cell biology* **14**, 416-429
- 5. Ingham, P. W. (2000) How cholesterol modulates the signal. Current biology: CB 10, R180-183
- 6. Taipale, J., Cooper, M. K., Maiti, T., and Beachy, P. A. (2002) Patched acts catalytically to suppress the activity of Smoothened. *Nature* **418**, 892-897
- 7. Denef, N., Neubuser, D., Perez, L., and Cohen, S. M. (2000) Hedgehog induces opposite changes in turnover and subcellular localization of patched and smoothened. *Cell* **102**, 521-531.
- 8. Hooper, J. E., and Scott, M. P. (1989) The Drosophila patched gene encodes a putative membrane protein required for segmental patterning. *Cell* **59**, 751-765
- 9. Marigo, V., Scott, M. P., Johnson, R. L., Goodrich, L. V., and Tabin, C. J. (1996) Conservation in hedgehog signaling: induction of a chicken patched homolog by Sonic hedgehog in the developing limb. *Development* 122, 1225-1233
- 10. Carstea, E. D., Morris, J. A., Coleman, K. G., Loftus, S. K., Zhang, D., Cummings, C., Gu, J., Rosenfeld, M. A., Pavan, W. J., Krizman, D. B., Nagle, J., Polymeropoulos, M. H., Sturley, S. L., Ioannou, Y. A., Higgins, M. E., Comly, M., Cooney, A., Brown, A., Kaneski, C. R., Blanchette-Mackie, E. J., Dwyer, N. K., Neufeld, E. B., Chang, T. Y., Liscum, L., Tagle, D. A., and et al. (1997) Niemann-Pick C1 disease gene: homology to mediators of cholesterol homeostasis [see comments]. *Science* 277, 228-231
- 11. Loftus, S. K., Morris, J. A., Carstea, E. D., Gu, J. Z., Cummings, C., Brown, A., Ellison, J., Ohno, K., Rosenfeld, M. A., Tagle, D. A., Pentchev, P. G., and Pavan, W. J. (1997) Murine model of Niemann-Pick C disease: mutation in a cholesterol homeostasis gene [see comments]. *Science* 277, 232-235
- 12. Kuwabara, P. E., and Labouesse, M. (2002) The sterol-sensing domain: multiple families, a unique role? *Trends in genetics : TIG* **18**, 193-201

- 13. Strutt, H., Thomas, C., Nakano, Y., Stark, D., Neave, B., Taylor, A. M., and Ingham, P. W. (2001) Mutations in the sterol-sensing domain of Patched suggest a role for vesicular trafficking in Smoothened regulation. *Current biology: CB* 11, 608-613.
- 14. Lu, X., Liu, S., and Kornberg, T. B. (2006) The C-terminal tail of the Hedgehog receptor Patched regulates both localization and turnover. *Genes Dev* **20**, 2539-2551
- 15. Corcoran, R. B., and Scott, M. P. (2006) Oxysterols stimulate Sonic hedgehog signal transduction and proliferation of medulloblastoma cells. *Proceedings of the National Academy of Sciences of the United States of America* **103**, 8408-8413
- 16. Bijlsma, M. F., Spek, C. A., Zivkovic, D., van de Water, S., Rezaee, F., and Peppelenbosch, M. P. (2006) Repression of smoothened by patched-dependent (pro-)vitamin D3 secretion. *PLoS biology* **4**, e232
- 17. Uhmann, A., Niemann, H., Lammering, B., Henkel, C., Fritsch, A., Prufer, N., Heb, I., Nitzki, F., Rosenberger, A., Dullin, C., Schraepler, A., Reifenberger, P. D., Schweyer, S., Pietsch, T., Strutz, F., Schulz-Schaeffer, W., and Hahn, H. (2011) Antitumoral effects of calcitriol in basal cell carcinomas involve inhibition of Hedgehog-signaling and induction of vitamin D receptor-signaling and differentiation. *Mol Cancer Ther* **10(11)**, 2179-2188
- 18. Nachtergaele, S., Whalen, D. M., Mydock, L. K., Zhao, Z., Malinauskas, T., Krishnan, K., Ingham, P. W., Covey, D. F., Siebold, C., and Rohatgi, R. (2013) Structure and function of the Smoothened extracellular domain in vertebrate Hedgehog signaling. *eLife* **2**, e01340
- 19. Nedelcu, D., Liu, J., Xu, Y., Jao, C., and Salic, A. (2013) Oxysterol binding to the extracellular domain of Smoothened in Hedgehog signaling. *Nature chemical biology* **9**, 557-564
- 20. Chen, J. K., Taipale, J., Cooper, M. K., and Beachy, P. A. (2002) Inhibition of Hedgehog signaling by direct binding of cyclopamine to Smoothened. *Genes Dev* **16**, 2743-2748
- 21. Robarge, K. D., Brunton, S. A., Castanedo, G. M., Cui, Y., Dina, M. S., Goldsmith, R., Gould, S. E., Guichert, O., Gunzner, J. L., Halladay, J., Jia, W., Khojasteh, C., Koehler, M. F., Kotkow, K., La, H., Lalonde, R. L., Lau, K., Lee, L., Marshall, D., Marsters, J. C., Jr., Murray, L. J., Qian, C., Rubin, L. L., Salphati, L., Stanley, M. S., Stibbard, J. H., Sutherlin, D. P., Ubhayaker, S., Wang, S., Wong, S., and Xie, M. (2009) GDC-0449-a potent inhibitor of the hedgehog pathway. *Bioorganic & medicinal chemistry letters* 19, 5576-5581
- 22. Chen, J. K., Taipale, J., Young, K. E., Maiti, T., and Beachy, P. A. (2002) Small molecule modulation of Smoothened activity. *Proceedings of the National Academy of Sciences of the United States of America* **99**, 14071-14076
- 23. Frank-Kamenetsky, M., Zhang, X. M., Bottega, S., Guicherit, O., Wichterle, H., Dudek, H., Bumcrot, D., Wang, F. Y., Jones, S., Shulok, J., Rubin, L. L., and Porter, J. A. (2002) Small-molecule modulators of Hedgehog signaling: identification and characterization of Smoothened agonists and antagonists. *Journal of biology* 1, 10
- 24. Dwyer, J. R., Sever, N., Carlson, M., Nelson, S. F., Beachy, P. A., and Parhami, F. (2007) Oxysterols are novel activators of the hedgehog signaling pathway in pluripotent mesenchymal cells. *The Journal of biological chemistry* **282**, 8959-8968
- 25. Nachtergaele, S., Mydock, L. K., Krishnan, K., Rammohan, J., Schlesinger, P. H., Covey, D. F., and Rohatgi, R. (2012) Oxysterols are allosteric activators of the oncoprotein Smoothened. *Nature chemical biology* **8**, 211-220
- 26. Uhmann, A., Niemann, H., Lammering, B., Henkel, C., Heß, I., Rosenberger, A., Dullin, C., Schraepler, A., Schulz-Schaeffer, W., and Hahn, H. (2012) Calcitriol Inhibits Hedgehog Signaling and Induces Vitamin D Receptor

- Signaling and Differentiation in the Patched Mouse Model of Embryonal Rhabdomyosarcoma. *Sarcoma* **2012**, 2012:357040
- 27. Ma, Y., Erkner, A., Gong, R., Yao, S., Taipale, J., Basler, K., and Beachy, P. A. (2002) Hedgehog-mediated patterning of the mammalian embryo requires transporter-like function of dispatched. *Cell* 111, 63-75
- 28. Xie, J., Aszterbaum, M., Zhang, X., Bonifas, J. M., Zachary, C., Epstein, E., and McCormick, F. (2001) A role of PDGFRalpha in basal cell carcinoma proliferation. *Proceedings of the National Academy of Sciences of the United States of America* **98**, 9255-9259
- 29. Boukamp, P., Petrussevska, R. T., Breitkreutz, D., Hornung, J., Markham, A., and Fusenig, N. E. (1988) Normal keratinization in a spontaneously immortalized aneuploid human keratinocyte cell line. *The Journal of cell biology* **106**, 761-771
- 30. Taipale, J., Chen, J. K., Cooper, M. K., Wang, B., Mann, R. K., Milenkovic, L., Scott, M. P., and Beachy, P. A. (2000) Effects of oncogenic mutations in Smoothened and Patched can be reversed by cyclopamine. *Nature* **406**, 1005-1009.
- 31. Xie, J., Murone, M., Luoh, S. M., Ryan, A., Gu, Q., Zhang, C., Bonifas, J. M., Lam, C. W., Hynes, M., Goddard, A., Rosenthal, A., Epstein, E. H., Jr., and de Sauvage, F. J. (1998) Activating Smoothened mutations in sporadic basal-cell carcinoma. *Nature* **391**, 90-92
- 32. Bartik, L., Whitfield, G. K., Kaczmarska, M., Lowmiller, C. L., Moffet, E. W., Furmick, J. K., Hernandez, Z., Haussler, C. A., Haussler, M. R., and Jurutka, P. W. (2010) Curcumin: a novel nutritionally derived ligand of the vitamin D receptor with implications for colon cancer chemoprevention. *The Journal of nutritional biochemistry* **21**, 1153-1161
- 33. Marklein, D., Graab, U., Naumann, I., Yan, T., Ridzewski, R., Nitzki, F., Rosenberger, A., Dittmann, K., Wienands, J., Wojnowski, L., Fulda, S., and Hahn, H. (2012) PI3K inhibition enhances doxorubicin-induced apoptosis in sarcoma cells. *PloS one* 7, e52898
- 34. Ecke, I., Rosenberger, A., Obenauer, S., Dullin, C., Aberger, F., Kimmina, S., Schweyer, S., and Hahn, H. (2008) Cyclopamine treatment of full-blown Hh/Ptch-associated RMS partially inhibits Hh/Ptch signaling, but not tumor growth. *Molecular carcinogenesis* 47, 361-372
- 35. Nitzki, F., Zibat, A., König, S., Wijgerde, M., Rosenberger, A., Brembeck, F. H., Carstens, P.-O., Frommhold, A., Uhmann, A., Klingler, S., Reifenberger, J., Pukrop, T., Aberger, F., Schulz-Schaeffer, W., and Hahn, H. (2010) Tumor stroma-derived Wnt5a induces differentiation of basal cell carcinoma of Ptch mutant mice via CaMKII. *Cancer research* 70, 2739-2748
- 36. Chou, T. C., and Martin, N. (2005) CompuSyn for Drug Combinations:PC Software and User's Guide: A Computer Program forQuantification of Synergism and Antagonism in Drug Combinations and the Determination of IC50 and ED50 and LD50 Values. *ComboSyn, Inc., Paramus, NJ*
- 37. Christakos, S., Dhawan, P., Ajibade, D., Benn, B. S., Feng, J., and Joshi, S. S. (2010) Mechanisms involved in vitamin D mediated intestinal calcium absorption and in non-classical actions of vitamin D. *The Journal of steroid biochemistry and molecular biology* **121**, 183-187
- 38. Rohatgi, R., Milenkovic, L., and Scott, M. P. (2007) Patched1 regulates hedgehog signaling at the primary cilium. *Science* **317**, 372-376

- 39. Myers, B. R., Sever, N., Chong, Y. C., Kim, J., Belani, J. D., Rychnovsky, S., Bazan, J. F., and Beachy, P. A. (2013) Hedgehog pathway modulation by multiple lipid binding sites on the smoothened effector of signal response. *Developmental cell* **26**, 346-357
- 40. Kim, J., Tang, J. Y., Gong, R., Kim, J., Lee, J. J., Clemons, K. V., Chong, C. R., Chang, K. S., Fereshteh, M., Gardner, D., Reya, T., Liu, J. O., Epstein, E. H., Stevens, D. A., and Beachy, P. A. (2010) Itraconazole, a commonly used antifungal that inhibits Hedgehog pathway activity and cancer growth. *Cancer cell* 17, 388-399
- 41. Kota, B. P., Allen, J. D., and Roufogalis, B. D. (2011) The effect of vitamin D3 and ketoconazole combination on VDR-mediated P-gp expression and function in human colon adenocarcinoma cells: implications in drug disposition and resistance. *Basic & clinical pharmacology & toxicology* **109**, 97-102
- 42. Muindi, J. R., Yu, W. D., Ma, Y., Engler, K. L., Kong, R. X., Trump, D. L., and Johnson, C. S. (2010) CYP24A1 inhibition enhances the antitumor activity of calcitriol. *Endocrinology* **151**, 4301-4312
- 43. Chen, T. C., Sakaki, T., Yamamoto, K., and Kittaka, A. (2012) The roles of cytochrome P450 enzymes in prostate cancer development and treatment. *Anticancer research* 32, 291-298
- 44. Lehmann, B. (1997) HaCaT cell line as a model system for vitamin D3 metabolism in human skin. *The Journal of investigative dermatology* **108**, 78-82
- 45. Eaton, S. (2008) Multiple roles for lipids in the Hedgehog signalling pathway. *Nature reviews. Molecular cell biology* **9**, 437-445
- 46. Hausmann, G., von Mering, C., and Basler, K. (2009) The hedgehog signaling pathway: where did it come from? *PLoS biology* 7, e1000146
- 47. Torroja, C., Gorfinkiel, N., and Guerrero, I. (2004) Patched controls the Hedgehog gradient by endocytosis in a dynamin-dependent manner, but this internalization does not play a major role in signal transduction. *Development* 131, 2395-2408
- 48. Bidet, M., Joubert, O., Lacombe, B., Ciantar, M., Nehme, R., Mollat, P., Bretillon, L., Faure, H., Bittman, R., Ruat, M., and Mus-Veteau, I. (2011) The hedgehog receptor patched is involved in cholesterol transport. *PloS one* **6**, e23834
- 49. Tang, J. Y., Xiao, T. Z., Oda, Y., Chang, K. S., Shpall, E., Wu, A., So, P. L., Hebert, J., Bikle, D., and Epstein, E. H., Jr. (2011) Vitamin d3 inhibits hedgehog signaling and proliferation in murine Basal cell carcinomas. *Cancer Prev Res (Phila)* **4**, 744-751
- 50. Hansdottir, S., Monick, M. M., Hinde, S. L., Lovan, N., Look, D. C., and Hunninghake, G. W. (2008) Respiratory epithelial cells convert inactive vitamin D to its active form: potential effects on host defense. *J Immunol* **181**, 7090-7099

#### **FOOTNOTES**

<sup>1</sup>To whom correspondence should be addressed: Anja Uhmann, Institute of Human Genetics, University Medical Center Goettingen, Heinrich-Dueker-Weg 12, 37073 Goettingen, Germany; Phone: +49 551 3914100; Fax: +49 551 3966580; email: <a href="mailto:auhmann@gwdg.de">auhmann@gwdg.de</a>

<sup>2</sup>Department Genome Analysis Centre, Institute for Experimental Genetics, Helmholtz Zentrum Muenchen, National Research Center for Environment and Health, Neuherberg, Germany

<sup>3</sup>Institute of Cellular and Molecular Immunology, University Medical Center Goettingen, Germany

<sup>4</sup>The abbreviations used are: Ptch, Patched1; Smo, Smoothened; ITZ, itraconazole; SSD, sterol-sensing-domain; wt, wildtype; 7TM, 7-transmembrane-domain; CRD, cysteine-rich-domain; CP, cyclopamine; SAG, Smoothened agonist;

20(S)OHC, 20(S)-hydroxycholesterol; Vdr, Vitamin D receptor; 25(OH)D<sub>3</sub>, 25-hydroxy vitamin D<sub>3</sub>; BD-CP, BODIPY-labeled CP, EtOH, ethanol; M2H, mammalian two hybrid; BrdU, 5-bromo-2'-deoxyuridine; BSA, bovine serum albumin; CRC, concentration-response curves; Shh-N-CM, Shh-N-conditioned medium; CoM, control medium; CDF, cumulative distribution function; PBST, PBS containing 0.1% Tween-20, SPE, solid phase extraction; MRM, multiple reaction monitoring; ESI, electrospray ionization; Fa, fractional inhibition; CI, combination index; Cyp27a1, vitamin D 25-hydroxylase; Cyp27b1, 1α-hydroxylase; MS, mass spectrometric analyses, VDR, vitamin D receptor; RXRα, retinoic X receptor alpha; BSA, bovine serum albumin; Cyp24a1, 25-hydroxy vitamin D<sub>3</sub>-24-hydroxylase; 1α,24,25(OH)<sub>3</sub>D<sub>3</sub>, 1α, 24, 25-trihydroxy vitamin D<sub>3</sub>; 24,25(OH)<sub>2</sub>D<sub>3</sub>, 24,25-dihydroxy vitamin D<sub>3</sub>; IC<sub>50</sub>, half maximal inhibitory concentration; ED50, half maximal effective dose

FIGURE 1: Loss of Ptch does not influence the vitamin D<sub>3</sub> metabolism but disturbs the calcitriol release from the cell. (a) MS-based intracellular quantification of the vitamin D<sub>3</sub> metabolites vitamin D<sub>3</sub> (solid line), 25(OH)D<sub>3</sub> (dashed line) and calcitriol (dotted line) in wt Ptch (left) and Ptch-(right) murine adult fibroblasts after 0.5, 1, 2, 4 and 6 h incubation with 10 μM vitamin D<sub>3</sub>. The data were normalized to the respective solvent-treated controls for each time point. (b) Schematic representation of the procedure for medium transfer experiments. Freshly trypsinized wt Ptch and Ptch<sup>-/-</sup> cells were calcitriol-loaded in a rotating 50 ml reaction tube filled with medium supplemented with 100 nM calcitriol for 1 h ("loading phase"). Solvent-supplemented medium served as control. After washing, the cells were plated in calcitriol-free medium for 4, 6 or 8 h, respectively ("conditioning phase"). The conditioned media were sterile-filtrated and transferred to M2H-transfected NIH/3T3 cells. Finally, dual-luciferase-assays were performed (see online methods). (c) Sensitivity of the reporter systems used to asses calcitriol-mediated Hh pathway inhibition (gray bars, left v-axis) and calcitriol-stimulated VDR/RXRα interaction (white bars, right v-axis). Data are shown from one representative experiment. For each reporter system values of solvent-treated cells were set to 1 (dashed line). Data are represented as mean +/- SEM. (d) Dual-luciferase-based analyses of M2H-transfected NIH/3T3 cells after 6 h incubation with conditioned media from calcitriol-loaded wt Ptch or Ptch- fibroblasts. The cells were loaded as described in (b). As a background-control calcitriol-loading was carried out using culture media without cells (no cell control). The conditioned medium was prepared in triplicates, the medium from no cell controls in duplicates. The treatment of the transfected cells was conducted in duplicates for each medium. Similar results were carried out after 4 and 8 h incubation of M2H-transfected NIH/3T3 cells with wt *Ptch* or *Ptch*<sup>-/-</sup> conditioned media (data not shown). Data represent normalized firefly/renilla luciferase activity. The solvent-loaded control for each cell line and timepoint was set to 1. All data represent at least 3 independent experiments represented as mean +/-SEM. \* p<0.05, \*\* p<0.01, \*\*\* p<0.001, \*\*\*\* p<0.0001 compared to solvent control; +p<0.05, +++p<0.001, ++++p<0.0001 compared to 0.5 h treatment.

FIGURE 2: Calcitriol prevents Smo accumulation in the primary cilia. (a) Relative quantification of *Gli1* expression of NIH/3T3 cells treated for 16 h with solvent 100 nM SAG, 100 nM calcitriol or 100 nM SAG and 100 nM calcitriol. Data are represented as mean +/-SEM of 2 independent experiments conducted in triplicates. \*\* p<0.01, \*\*\*\* p<0.0001. (b-e) Immunofluorescence-based analyses of Smo accumulation in the primary cilia of (b and c) NIH/3T3 cells treated for 16 h with solvent, 100 nM calcitriol, 100 nM SAG, 100 nM SAG and 1 μM vismodegib (SAG/vismo) or 100 nM SAG and 100 nM calcitriol (SAG/calcitriol) and (d and e) *Ptch*<sup>-/-</sup> cells treated for 16 h with solvent, 10 or 100 nM calcitriol or 1 μM vismodegib (vismo). (c and e) Representative images of anti-acetylated tubulin (AT, green) and anti-Smo (red) antibodies stained cells. Nuclei were visualized with DAPI (blue). Top rows, images of entire cells in 1000x magnification; bottom rows, magnification of boxed regions (white squares) containing cilia. (b and d) Percentages of Smo containing primary cilia relative to (b) NIH/3T3 cells treated with 100 nM SAG (100%) or (d) to solvent-treated *Ptch*<sup>-/-</sup> cells (100%). Numbers indicate the total numbers of counted Smo positive cilia/all counted cilia. At least all primary cilia in 6 visual fields of three independent experiments conducted in duplicates were counted. Data are represented as mean +/-SEM. \*\*\*\* p<0.0001 compared to (b) SAG-treated NIH/3T3 or (d) solvent-treated *Ptch*<sup>-/-</sup> cells.

FIGURE 3: Calcitriol-mediated inhibition of Smo<sup>ACRD</sup>. (a and b) Dual-luciferase-based analyses of Hh pathway activation of untransduced and wt Smo (Smo<sup>wt</sup>) or Smo<sup>ACRD</sup> (carrying a CRD deletion) expressing Shh light II cells treated with (a) Smo-agonist (SAG) or (b) Shh-N-CM. (c and d) Dual-luciferase-based analyses of Hh pathway inhibition by calcitriol or cyclopamine (CP) of (c) untransduced SAG or Shh-N-CM-induced Shh light II cells and (d)

 $Smo^{wt}$  or  $Smo^{\Delta CRD}$  transduced Shh light II cells. Values of SAG or Shh-N-CM-induced cells in (c) and solvent-treated cells in (d) were set to 100%. Data represent normalized firefly/renilla luciferase activity. (e) Relative quantification of *Gli1* expression levels of untransduced,  $Smo^{wt}$  or  $Smo^{\Delta CRD}$  transfected  $Smo^{-/-}$  fibroblasts to analyze basal expression levels of *Gli1*. (f and g) Relative quantification of *Gli1* expression levels of (f)  $Smo^{wt}$  or  $Smo^{\Delta CRD}$  stable transfected  $Smo^{-/-}$  fibroblasts and (g) SMO or SMO-M2 transiently transfected  $Smo^{-/-}$  cells treated with calcitriol or  $Smo^{-/-}$  expression levels were normalized to  $Smo^{-/-}$  expression levels were normalized to  $Smo^{-/-}$  transfected  $Smo^{-/-}$  cells treated with calcitriol or  $Smo^{-/-}$  expression levels were normalized to  $Smo^{-/-}$  expression levels. Solvent treated controls were set to 1. All data represent at least 3 independent experiments measured in triplicates represented as mean  $Smo^{-/-}$  expression levels.  $Smo^{-/-}$  expression levels were set to 1. All data represent at least 3 independent experiments measured in triplicates represented as mean  $Smo^{-/-}$  expression levels.

FIGURE 4: Enhanced antitumoral effects of combined calcitriol/ITZ treatment in the BCC cell line ASZ001. Relative quantification of (a, d and g) *Gli1* or (b, e and h) *Cyp24a1* expression levels and (c, f and i) BrdU incorporation-assay of ASZ001 cells after treatment with (a-c) 10 nM calcitriol (cal) and 1 μM itraconazole (ITZ), (d-f) 10 nM calcitriol (cal) and 5 μM cyclopamine (CP) or (g-i) 5 μM CP and 1 μM itraconazole (ITZ) alone or in combination. Experiments shown in (a-c and g-i) were conducted in media supplemented with 1.5% BSA, in (d-f) in media supplemented with 2% FCS. Gene expression levels were normalized to *18S* rRNA expression levels. The respective solvent-controls for each experiment were set to 1. All data represent at least 3 independent experiments measured in triplicates. The data are represented as mean +/-SEM; \*, p<0.05; \*\*, p<0.01; \*\*\*\*, p<0.001.

FIGURE 5: ITZ does not inhibit the enzymatic activity of the 24-hydroxylase in ASZ001 cells. MS-based intracellular quantification of the vitamin  $D_3$  metabolites (a) 25(OH) $D_3$ , (b) 24,25(OH) $D_3$  and (c) calcitriol in ASZ001 cells after 6 h incubation with (a and b) 2 μM 25(OH) $D_3$  or (c) 100 nM calcitriol alone or in combination with 2 μM itraconazole (ITZ). The data were normalized to the respective solvent-treated control. The experiments were performed at least three times in triplicates. Each point represents the mean +/- SEM of all experiments. \* p<0.05, \*\* p<0.01 compared to solvent control.

FIGURE 6: Calcitriol synergizes with ITZ in inhibition of Hh signaling activity. (a-c, e and f) Concentration-response curves of calcitriol in the presence of the Hh-inhibitors (a) cyclopamine (CP), (b) vismodegib (vismo), (c) itraconazole (ITZ) or the Hh activators (e) Smo-agonist (SAG), (f) 20(S)-hydroxycholesterol (20(S)OHC). Data represent normalized firefly/renilla luciferase activity. All data represent at least 3 independent experiments measured in triplicates represented as mean +/-SEM. (d) Fa-CI-Plot was generated by calculating the combination index (CI) over the range of the fractional inhibition (Fa) of the experimental data shown in (c). Shown are the CI-values and linear regression of Hh signaling inhibition triggered by 0.5, 2.5 and 5 nM calcitriol (circles, squares, triangles, respectively) combined with 0.1, 0.5 or 2 μM ITZ plotted against the respective Fa. Slopes of 0.5 nM and 2.5 nM (p=0.044) as well as 0.5 nM and 5.0 nM calcitriol (p=0.023) are statistically different. CI>1, antagonism; C=1, additive (threshold) CI<0.7, synergism; CI<0.3, strong synergism (36).

FIGURE 7: Calcitriol binds to a site distinct from the CP binding site. Direct competition-assays of 10 nM BODIPY-labeled cyclopamine (BD-CP) and the Smo-modulators (a) unlabeled cyclopamine (CP), (b) itraconazole (ITZ), (c) calcitriol (cal) and (d) 20(S)-hydroxycholesterol (20(S)OHC) were performed in tetracycline-induced conditional Smo-overexpressing HEK293S cells (induced) as described (24). Solvent-treated, single CP, ITZ, calcitriol or (20(S)OHC)-treated cells and BD-CP-treated, uninduced HEK293S cells (not induced) served as negative controls. Data acquisition was conducted as described in experimental procedures. BD-CP single-treatments were set to 100. All data represent at least 3 independent experiments measured in duplicates represented as mean +/-SEM. \* p<0.05;\*\*\* p<0.01, \*\*\*\*\* p<0.0001.

TABLE 1: IC<sub>50</sub> of calcitriol on inhibition of Hh signaling activity in combination with Smo-modulators.

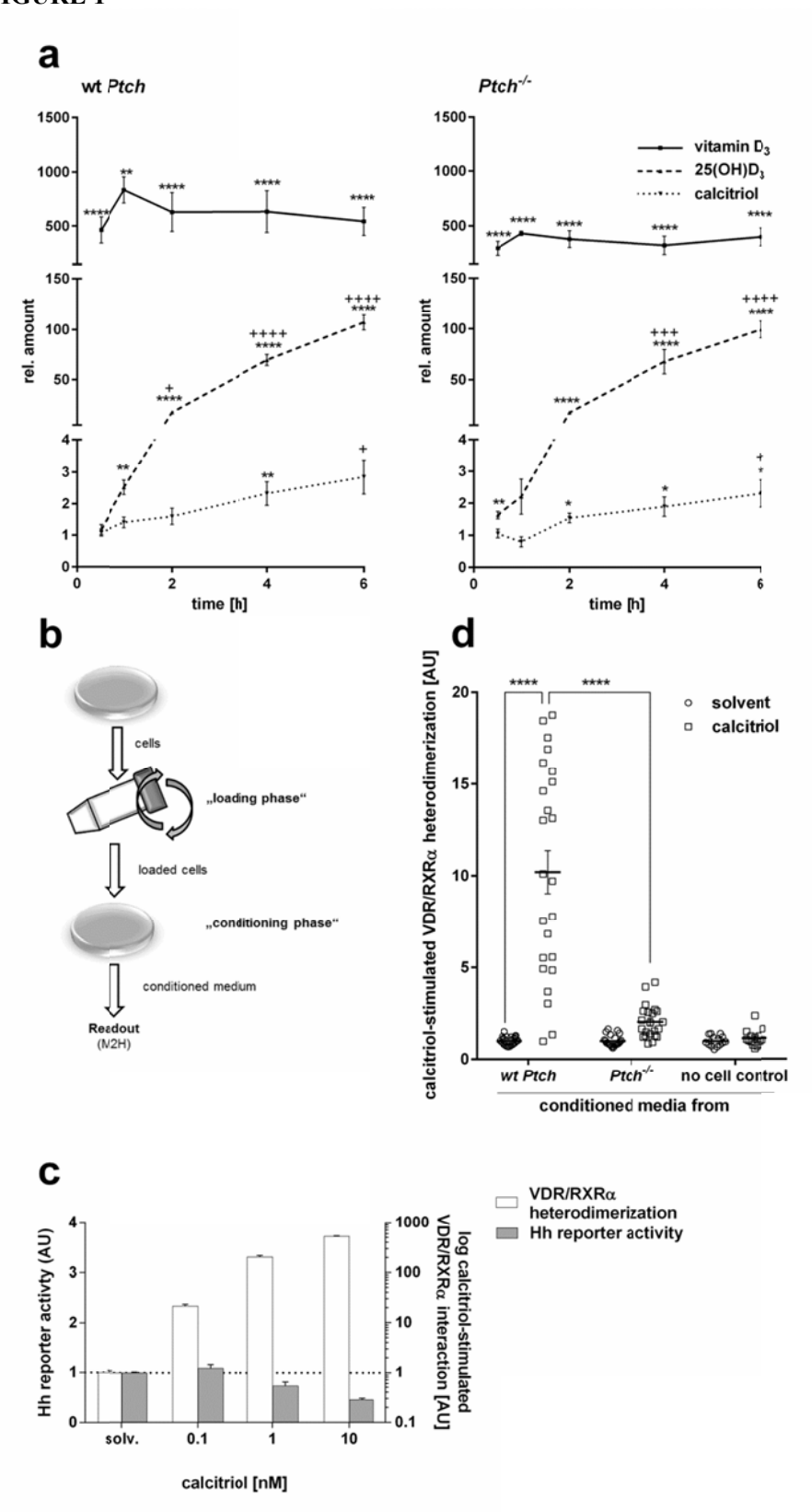
50		,		
	IC <sub>50</sub> of calcitriol [nM]	p value		
without CP	0.55			
0.1 μM CP	0.77			
0.2 μM CP	1.18	0.2014		
0.3 μΜ CP	0.45			
0.5 μM CP	1.01			
without vismo	0.46			
2.5 nM vismo	0.18	0.0739		
10 nM vismo	0.67	0.0739		
40 nM vismo	0.92			
without ITZ	1.02			
$0.1~\mu M~ITZ$	0.44	0.0004		
$0.5~\mu M~ITZ$	0.27	0.0004		
2 μM ITZ	0.13			
without SAG	n. d.			
5 nM SAG	1.38	0.7716		
50 nM SAG	1.50	0.7710		
100 nM SAG	1.14			
without 20(S)OHC	n. d.			
2 μM 20(S)OHC	0.13	0.3725		
5 μM 20(S)OHC	1.36	0.3723		
10 μM 20(S)OHC	1.11			

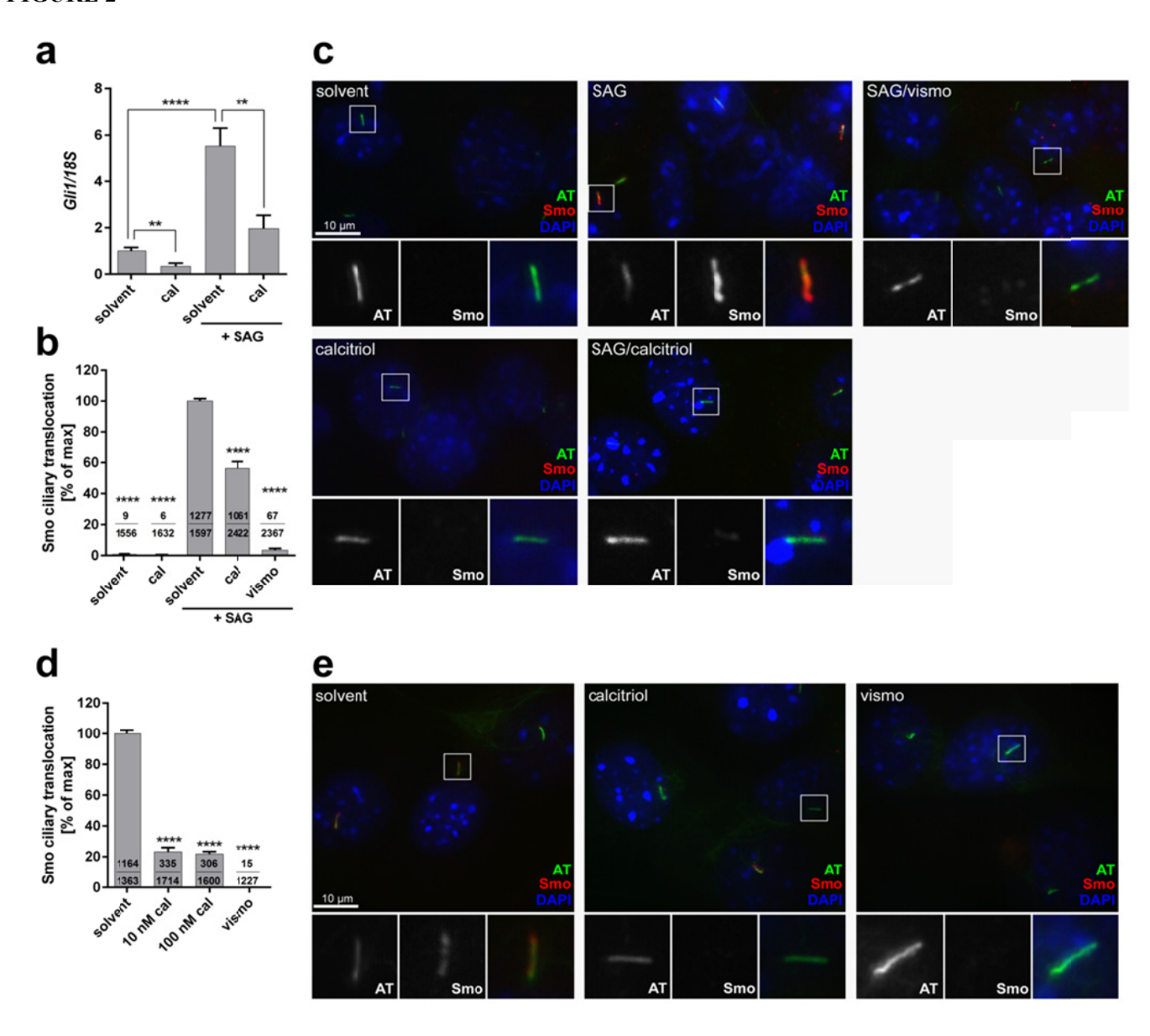
The half maximal inhibitory concentration ( $IC_{50}$ ) of calcitriol on Hh signaling activity in combination with cyclopamine (CP), vismodegib (vismo), itraconazole (ITZ), Smo-agonist (SAG) or 20(S)-hydroxycholesterol (20(S)OHC) was calculated from the experiments shown in Figure 6 as described in experimental procedures. To detect significant differences of the  $IC_{50}$  of single calcitriol and combined calcitriol/Smo-modulators treatments extra sum-of-squares F tests were conducted. n.d., not determined.

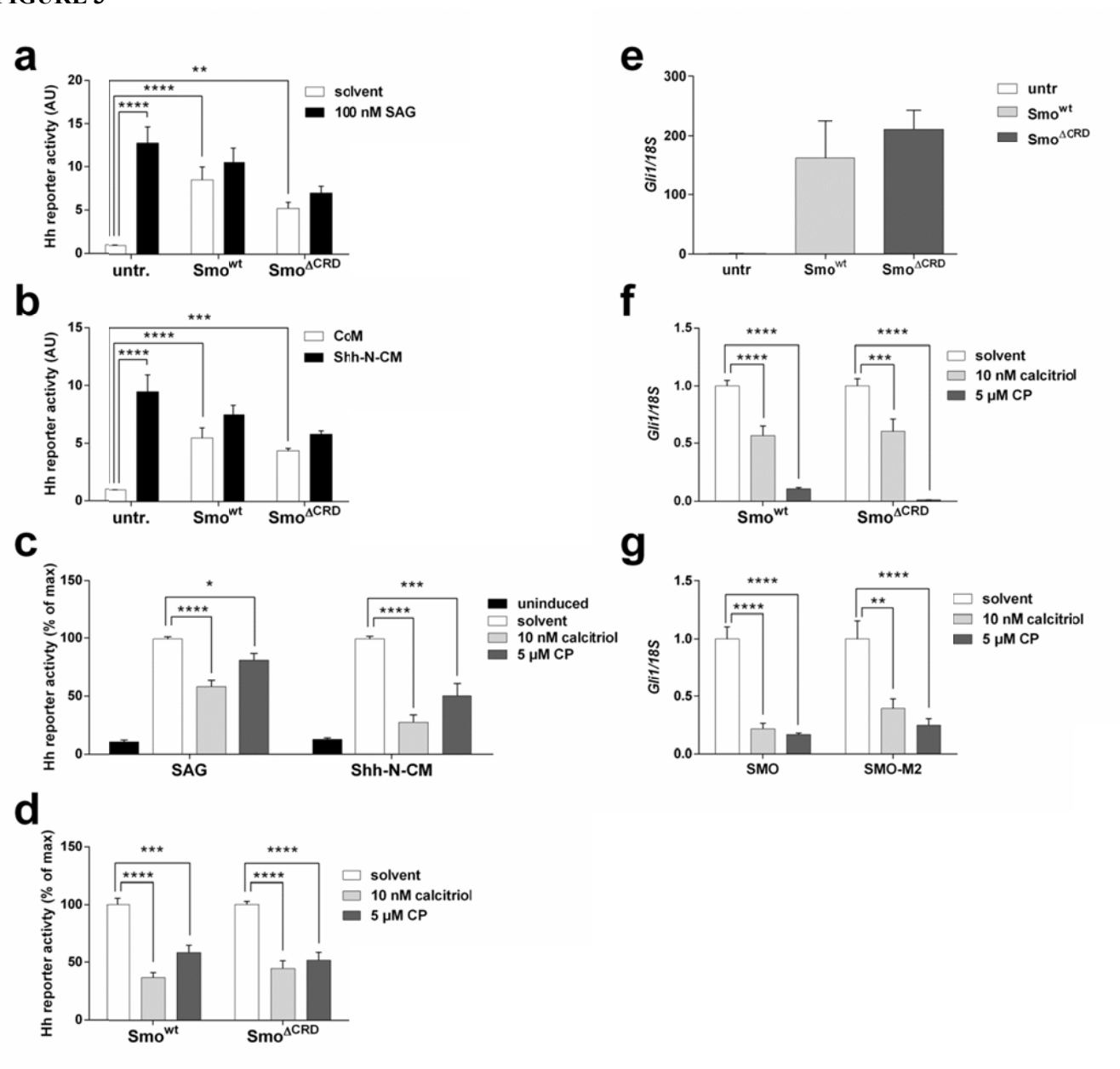
TABLE 2:  $IC_{50}$  of CP, vismodegib and ITZ and  $EC_{50}$  of SAG and 20(S)OHC on Hh signaling activity in combination with calcitriol.

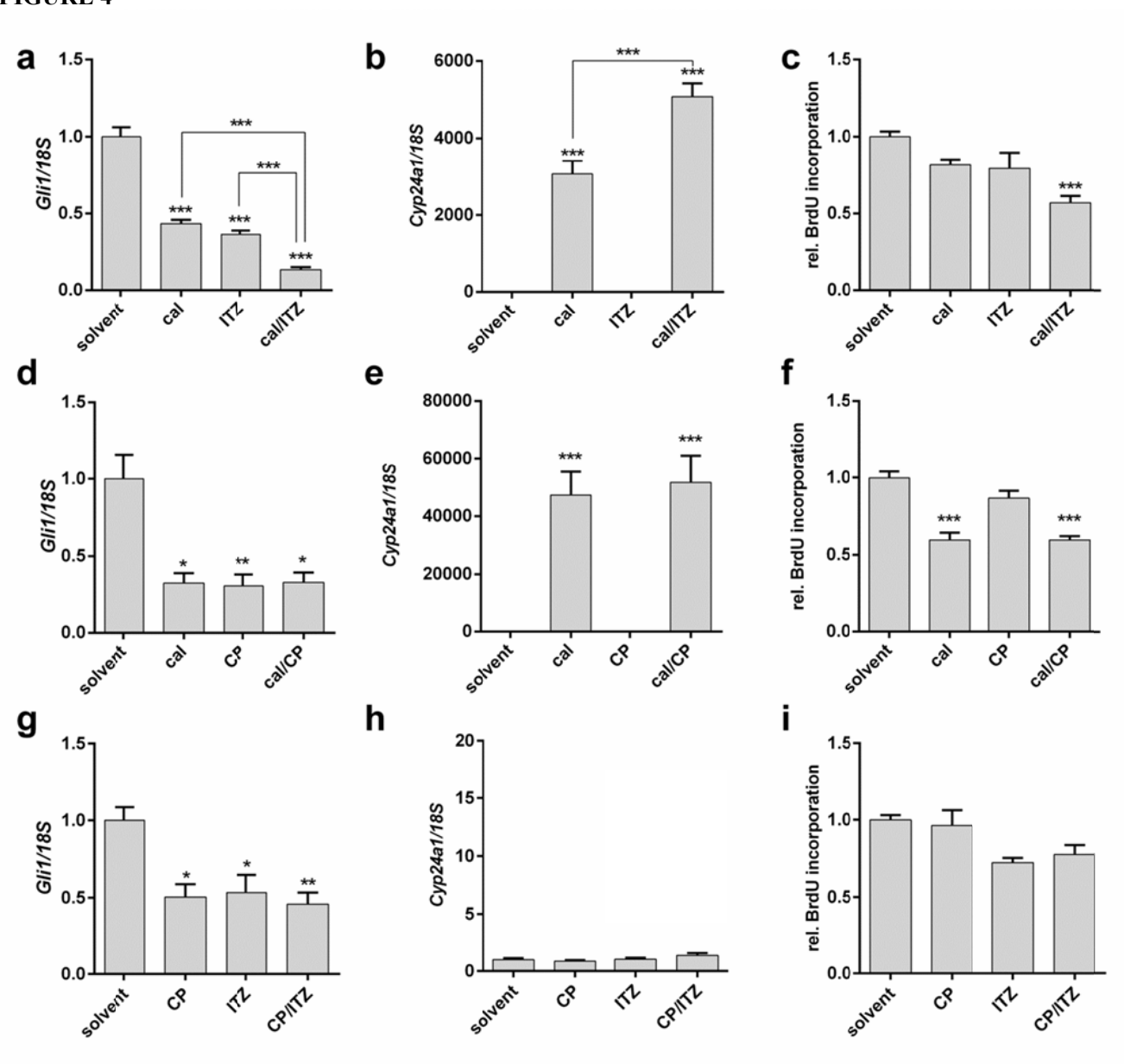
	IC <sub>50</sub> CP [μM]	IC <sub>50</sub> vismo [nM]	IC <sub>50</sub> ITZ [μM]	EC <sub>50</sub> SAG [nM]	EC <sub>50</sub> 20(S)OHC [μΜ]
without calcitriol	0.25	6.40	0.81	5.40	5.16
0.1 nM calcitriol	0.33	3.57	0.43	6.46	4.98
1 nM calcitriol	0.35	4.13	0.32	6.07	4.55
10 nM calcitriol	0.55	4.20	0.59	5.03	4.66
p value	0.0758	0.1788	0.0075	0.6268	0.3725

The half maximal inhibitory concentration (IC $_{50}$ ) of cyclopamine (CP), vismodegib (vismo) or itraconazole (ITZ) and half maximal effective concentration (EC $_{50}$ ) of Smo-agonist (SAG) or 20(S)-hydroxycholesterol (20(S)OHC) in combination with calcitriol on Hh signaling activity were calculated as described in experimental procedures. To detect significant differences of the IC $_{50}$  or EC $_{50}$  of single and combined treatments extra sum-of-squares F tests were conducted.

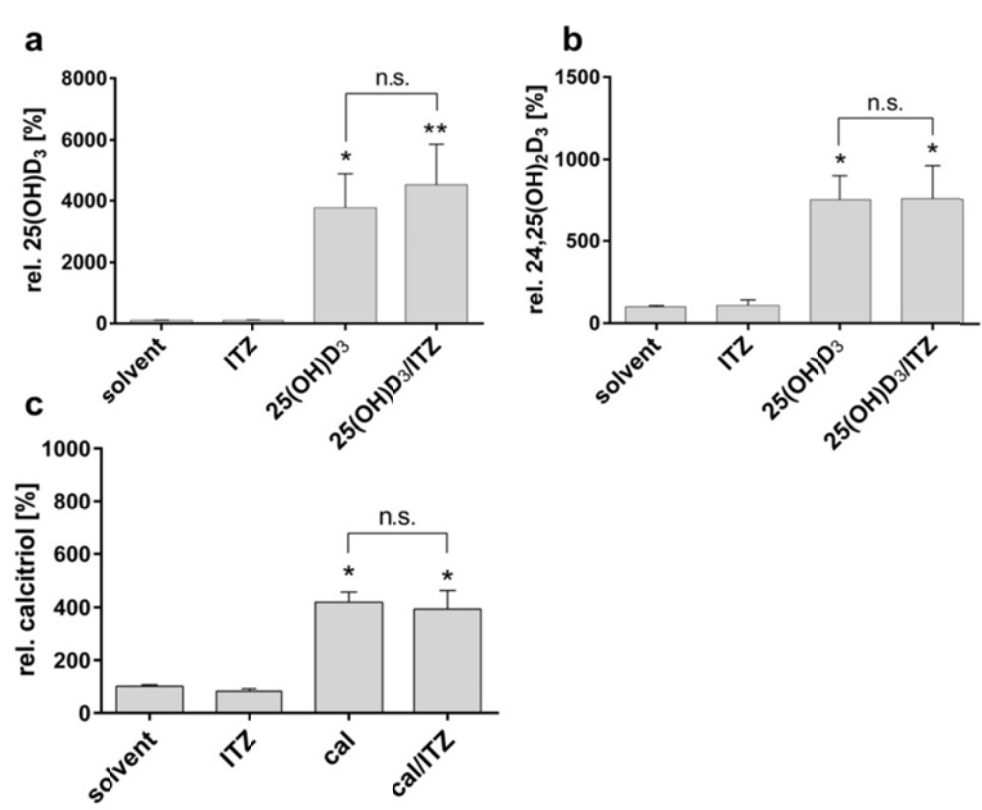


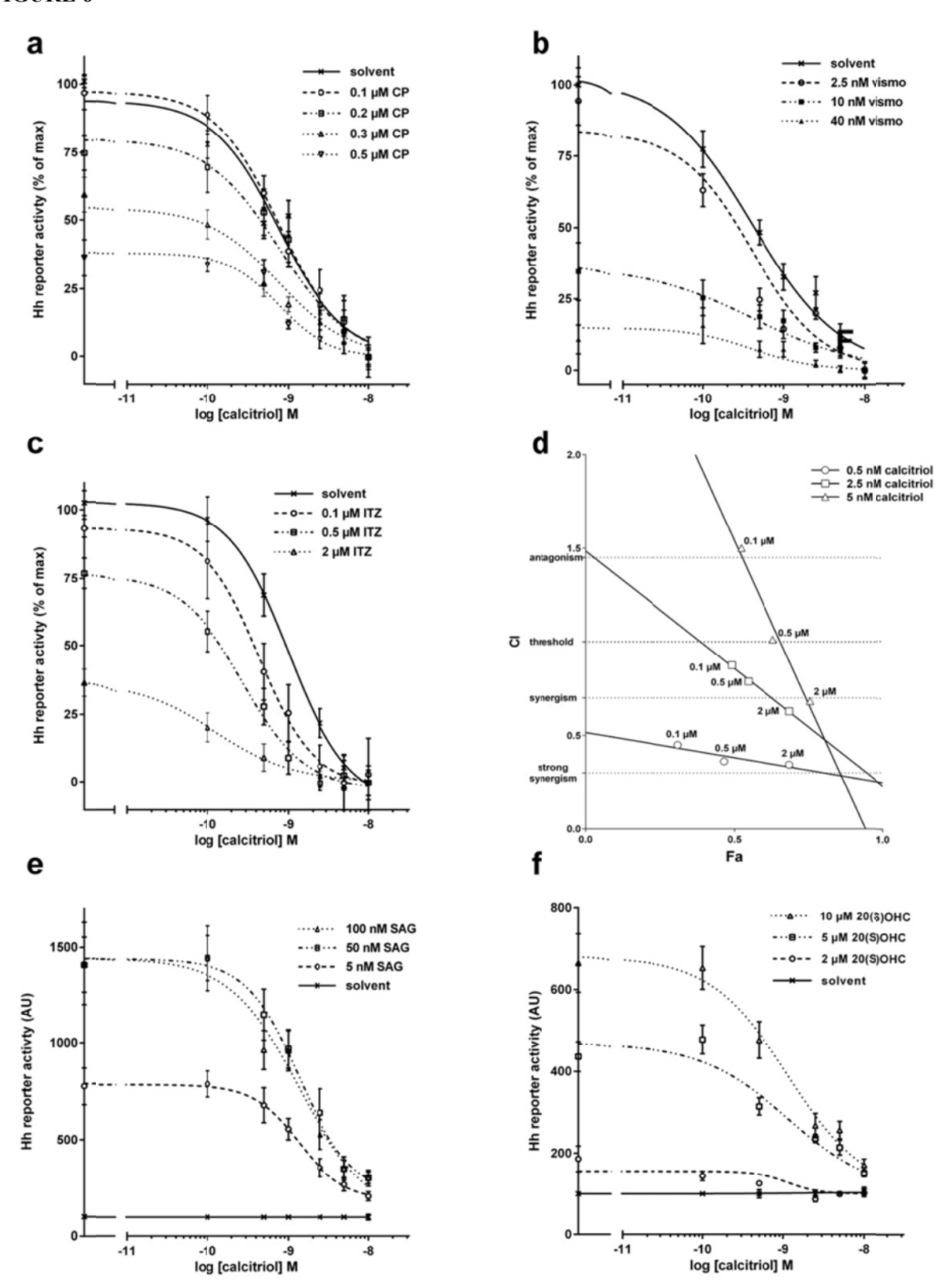


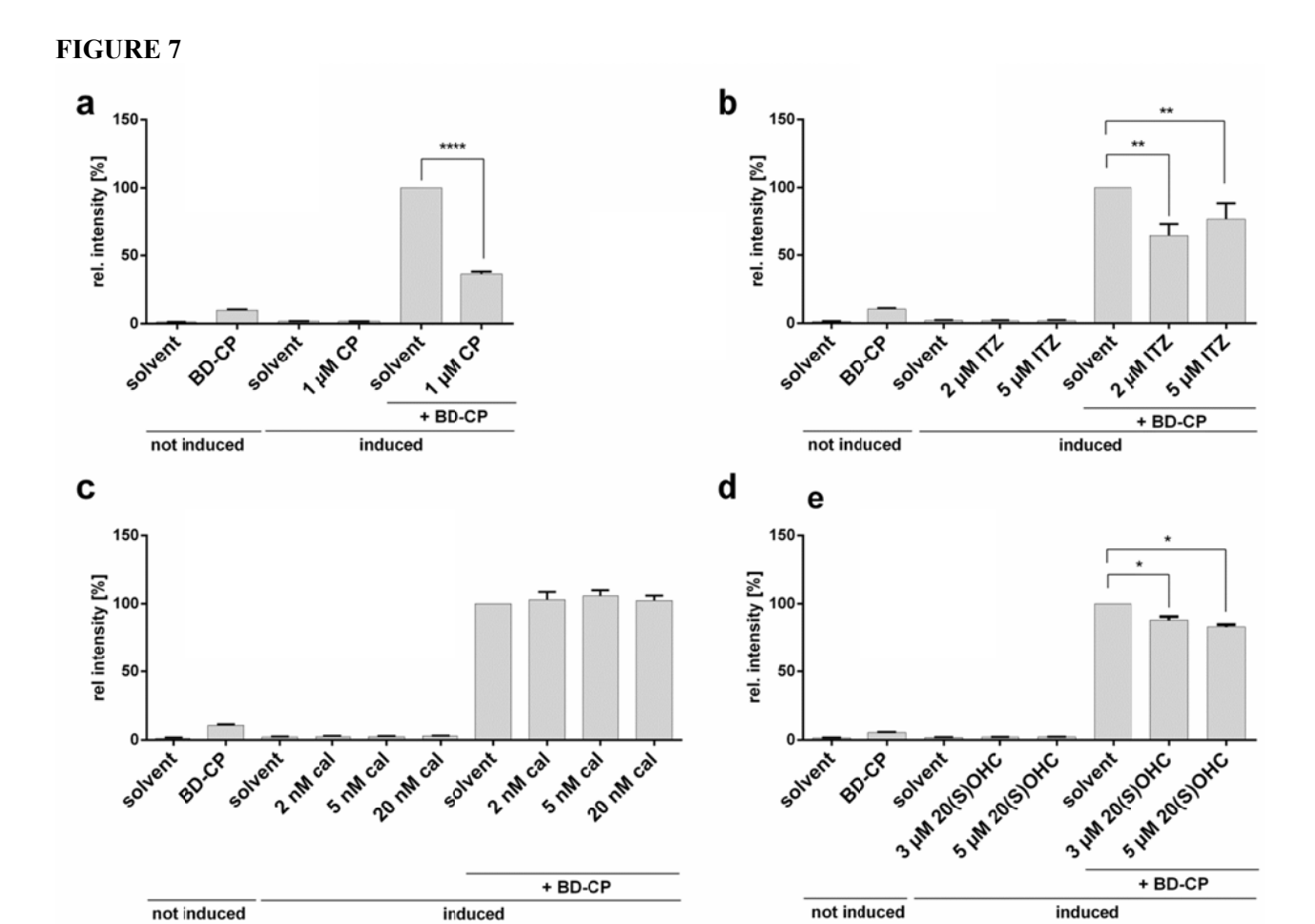














### Signal Transduction:

A functional and putative physiological role of calcitriol in Patched1/Smoothened interaction



Benedikt Linder, Susanne Weber, Kai Dittmann, Jerzy Adamski, Heidi Hahn and Anja Uhmann J. Biol. Chem. published online June 30, 2015

Access the most updated version of this article at doi: 10.1074/jbc.M115.646141

Find articles, minireviews, Reflections and Classics on similar topics on the JBC Affinity Sites.

### Alerts:

- When this article is cited
- · When a correction for this article is posted

Click here to choose from all of JBC's e-mail alerts

This article cites 0 references, 0 of which can be accessed free at http://www.jbc.org/content/early/2015/06/30/jbc.M115.646141.full.html#ref-list-1